GEOPHYSICAL RESEARCH LETTERS, VOL. 28, NO. 22, PAGES 4235-4238, NOVEMBER 15, 2001

Interannual prediction of the Paraná river

Andrew W. Robertson,[1] and Carlos R. Mechoso

Department of Atmospheric Sciences, University of California, Los Angeles, California.

Norberto O. Garcia

Facultad de Ingeniería y Ciencias Hídricas, Universidad Nacional del Litoral, Santa Fe, Argentina.

Abstract. Interannual-to-decadal predictability of the Paraná river in South America is investigated by extracting near-cyclic components in summer-season streamflows at Corrientes over the period 1904–1997. It is found that oscillatory components with periods of about 2–5, 8 and 17 years are accompanied by statistically significant changes in monthly streamflow. Autoregressive predictive models are constructed for each component. Cross-validated categorical hindcasts based on the 8-yr predicted component are found to yield some skill up to four years in advance for below-average flows. A prediction based upon the 8- and 17-yr components including data up to 1999 suggests increased probability of below-average flows until 2006.

1. Introduction

The possibility of predicting river flows months and even years in advance is of great interest to regional economies that depend heavily on hydroelectricity and irrigation. This has motivated development of methods for streamflow prediction that use climatic information, such as the El Niño-Southern Oscillation (ENSO) (e.g., [*Valdés et al.*, 1999], [*Dettinger et al.*, 1999]).

Time series analysis can be a powerful approach to streamflow prediction, provided narrow-band signals that yield information about the underlying dynamics can be identified robustly [*Ghil et al.*, 1991]. The cyclic nature of ENSO, though irregular, has been exploited to make statistical predictions by using singular spectrum analysis (SSA) [*Vautard and Ghil*, 1989], a variant of principal component analysis, together with the maximum entropy method (MEM) to build autoregressive linear prediction models based on underlying oscillatory components [*Keppenne and Ghil*, 1992]. At a lead time of 6 months, SSA-MEM hindcasts of sea surface temperature (SST) anomalies over the eastern equatorial Pacific yield an overall correlation skill against observed anomalies of 0.75 for the decade 1984–93 [*Ghil and Jiang*, 1998].

This paper examines near-cyclic components and their interannual predictability in the Paraná, the largest river in the Plata river basin that covers a vast area (3.6×10^6 km^2) of subtropical South America. It is bounded by the Andes to the west and the Atlantic Ocean to the east, extending southward from near 15°S to the Plata river estuary near 35°S. We use monthly data for the summer months January–March (JFM) for the period 1904–1997, recorded at Corrientes (56°W, 27°S), which is located just downstream of the major Paraná-Paraguay river confluence.

In addition to an ENSO signal in the Paraná [*Depetris et al.*, 1996], a near-decadal cycle that is associated with SST anomalies over the northern tropical Atlantic has been identified [*Robertson and Mechoso*, 1998], as well as a 15–18-yr cycle in the north-south difference between streamflows of the Uruguay and Negro rivers to the south, and the Paraná and Paraguay rivers to the north [*Robertson and Mechoso*, 2000]. This latter cycle appears to be associated with changes in the intensity of the South American summer monsoon and the southward moisture transport by the low-level jet along the eastern slopes of the Andes.

2. Singular spectrum analysis

SSA is based on an eigenvector decomposition of the Toeplitz autocorrelation matrix into empirical orthogonal functions (EOFs) which form data-adaptive band-limited filters, consisting of pairs of eigenelements. A significance test for the reliable identification of oscillatory pairs can be made against a red noise null-hypothesis using a Monte Carlo method [*Allen and Smith*, 1996]. One can then reconstruct that part of the time series associated with an oscillatory pair by summing the products of its two EOFs (k_1, k_2) with their respective principal components, yielding a partial sum of *reconstructed components* (RCs k_1–k_2) [*Vautard et al.*, 1992]. We applied SSA to JFM averages of the Corrientes 1904–1997 series using the SSA-MTM Toolkit of [*Dettinger et al.*, 1995].

Figure 1 shows the SSA spectrum, constructed using a window-width of $M = 30$ yrs. The two leading EOF pairs account for 16.0% and 13.4% of the variance, respectively. Application of MEM to the corresponding RCs gives periods of 8.1 and 17.0 yrs respectively. No trend is identified in the JFM-averaged flows. The statistical significance of these results against a first-order autoregressive process is only moderate. Nevertheless, these periods match those found with higher significance in previous studies [*Robertson and Mechoso*, 1998, 2000], and they are robust to changes in M and found in annual averages. There are also moderate-variance pairs of EOFs in the 2–5-yr period range.

Partial reconstructions in terms of RCs are plotted in Fig. 2. Here we have used window-widths of $M = 30$ for the 17-yr and $M = 20$ for the 8-yr pair, in order to minimize M in each case. We compute the "ENSO" RCs by first subtracting RCs 1–4 of a preliminary SSA with $M = 20$ to "detrend" the time

---

[1] Also at Institute of Geophysics and Planetary Physics (IGPP), UCLA.

Copyright 2001 by the American Geophysical Union.

Paper number 2000GL012197.
0094-8276/01/2000GL012197$05.00

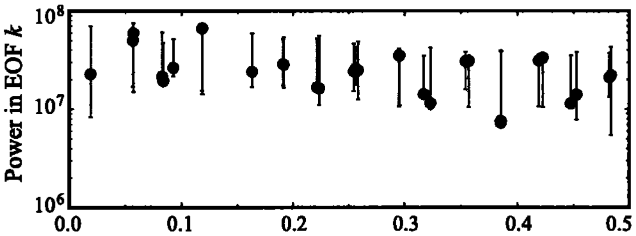

Figure 1. SSA eigenvalue spectrum and 90% red-noise confidence interval, computed using a Monte Carlo method with 1000 realizations.

series, and then apply SSA again to the detrended series with $M = 15$. The leading four EOFs so obtained have periods of 5.4 and 3.5 yrs and account for 39.3% of the detrended series. A 3.3-yr peak has been previously identified in the Paraná [*Depetris et al.*, 1996], and both periods have counterparts in the Uruguay and Negro rivers that are associated with ENSO ([*Mechoso and Perez-Iribarren*, 1992], [*Robertson and Mechoso*, 1998]).

3. Monthly flows versus RC category

The RC sums in Fig. 2 account individually for modest amounts of variance. Table 1 is a contingency table of *monthly* stream-flow categories, as a function of indices defined by each RC sum. This table measures the upper-bound on predictive skill that would be obtained if the RCs were *perfectly* predictable, assuming stationary statistics. Monthly stream flows are divided into below normal (1–30%-ile of historical data), normal (31–70%-ile), and above normal flows (71–100%-ile). The RC indices are divided according to their standard deviation σ into negative (RC $< -\sigma$), weak ($-\sigma \leq$ RC $\leq \sigma$) and positive (RC $> \sigma$) categories. The entries in Table 1 are probabilities in percent, with expected values of 30% (top rows) 40% (middle) and 30% (bottom). Statistical significance is assessed using a simple Monte Carlo scheme in which the years in the streamflow record are permutated randomly 100 times.

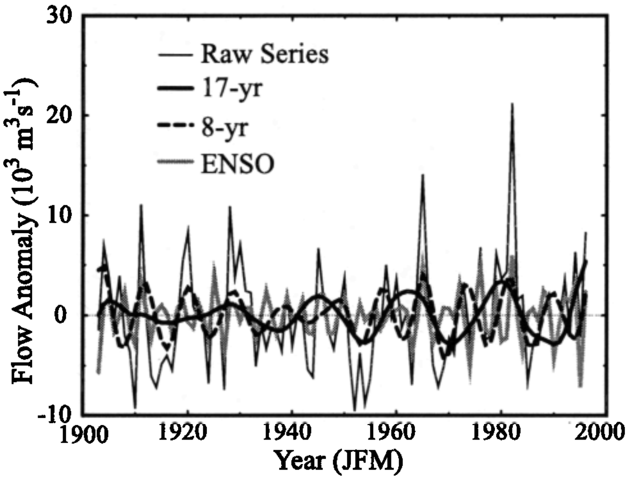

Figure 2. Partial reconstructions (RC sums) for the 17-yr (RCs 1–2), 8-yr (RCs 3–4), and ENSO components (RCs 1–4 of detrended series), together with the unfiltered original series.

Table 1. Probabilities (%) of monthly streamflow for each RC category, defined in Fig. 2. Bold-face values are significant at the 95% level.

Flow category		RC index category		
		$RC < -\sigma$	$-\sigma \leq RC \leq \sigma$	$RC > \sigma$
1 – 30%	ENSO	**59**	29	**08**
	8-yr	**48**	30	**11**
	17-yr	**52**	28	**15**
31 – 70 %	ENSO	31	**44**	22
	8-yr	41	41	31
	17-yr	28	43	40
71 – 100%	ENSO	**10**	28	**69**
	8-yr	**11**	28	**57**
	17-yr	20	29	46

Higher probabilities of above- (below-) normal *monthly* flows clearly do occur when each RC index is in its positive (negative) category. Except for the above-normal/17-yr cases (bottom row), all these are statistically significant. By contrast, the probabilities for the near-normal streamflow category are rarely significantly different from the expected value of 40%.

4. Hindcast RC predictions

The near-cyclic nature of the RCs implies predictability [*Vautard et al.*, 1992]. We use standard autoregressive linear prediction (LP) methodology (e.g. [*Press et al.*, 1992]) to advance the RCs forward in time. We firstly define a $N_T = 40$-yr long training time series starting in 1904, with the remainder of the 94-yr series used for validation; 40 consecutive 20-yr hindcasts are then made by shifting the training series forward one year each time.

With an SSA window of $M = 30$ yrs needed to isolate the 17-yr component, $N_T = 40$ yrs is found to be too short for obtaining robust RCs. We assume therefore, to begin with, that the near-periodicities are *stationary* in time, and compute the EOFs from the entire 94-yr length of the time series. The RCs are then obtained by projecting these fixed EOFs onto each $N_T = 40$-yr training time series. Figure 3 shows anomaly correlation hindcast skills for each of the three RC sums, together with persistence hindcasts made by persisting the lead-0 hindcast. Correlations are made against the respective RC sum derived from the entire time series. Both the 8- and 17-yr RCs show anomaly correlations exceeding 0.6 up to lead times of at least 8 yrs. The skill of the ENSO RCs is small, even at 1-yr lead, consistent with ENSO prediction studies, e.g. [*Ghil and Jiang*, 1998].

Although we are validating in Fig. 3 against the RC time series themselves, rather than the raw data, several factors contribute to loss of skill. Firstly, the RCs become uncertain near the ends of the training time series [*Vautard et al.*, 1992] so that the lead-0 anomaly correlation score is not unity. Secondly, the RCs describe non-sinusoidal oscillations that are modulated in amplitude and phase over time.

The major caveat of Fig. 3 is the use of "in sample" estimates of the EOFs, so that the training and validation series are not strictly independent. These hindcast skill scores measure the degree to which the *phase* of the RC is predictable, and give an upper bound on the degree of predictability.

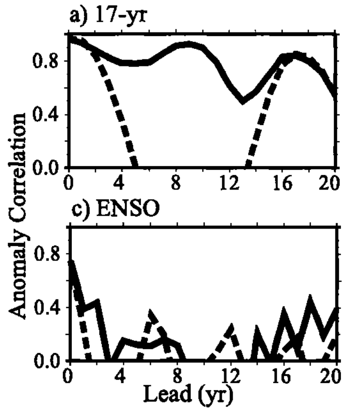

Figure 3. Anomaly correlation hindcast skills (solid line) for each RC sum in Fig. 2, verifying against the respective RC sum itself. Dashed line: persistence hindcast from the lead-0 RC hindcast. MEM is used to compute 10 LP coefficients.

5. Hindcast categorical prediction skill

Taken together, Table 1 and Fig. 3 suggest useful probabilistic categorical predictions may be possible. This is next quantified in terms of the equitable threat score (ETS, [*Schaefer*, 1990]) of categorical hindcasts based on each RC sum. To obtain a true measure of skill, we now completely separate the training and validation parts of the flow series. The RCs are thus obtained from the training part of the time series *alone*, and we validate against the raw data from the subsequent part of the series. The ETS measures the number of correct categorical predictions ("hits") in excess of those that would verify by chance, normalized by the total number of "threats" (hits, misses and false alarms) that would not have been foreseen by chance. The ETS is 0 for a by-chance result, and reaches 1 when events and forecasts of events are perfectly correlated.

We found that statistically significant ETS scores can be obtained from the 8-yr RC pair (Fig. 4) for below-average (1–40%-ile) seasonal-mean flows. For the parameters chosen (see caption), these predictions are consistently skillful up to four years in advance, while no skill was found for above-normal (61–100%-ile) flows. Different choices of M and N_T yield broadly similar results. The ENSO and 17-yr components do not yield significant ETS scores unless the entire time series is used to determine the EOFs.

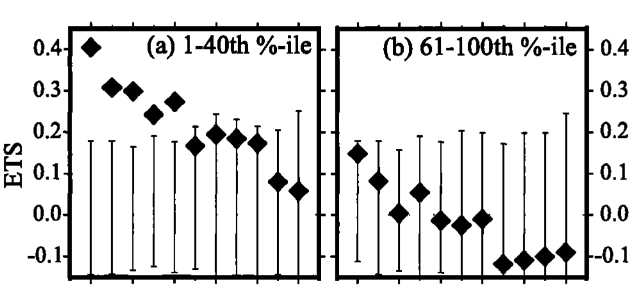

Figure 4. Equitable threat scores (ETS) for 8-yr RC out-of-sample hindcasts, for (a) below-normal JFM flow averages, and (b) above-normal ones (M = 30, 5 LP coefficients). Vertical bars indicate the 90% confidence interval of sampling variability computed by permutating the validation series 1000 times. The results shown are an average over (up to) 37 predictions at each lag, with the first prediction made from a training time series ending in 1960, and the final validation year being 1999.

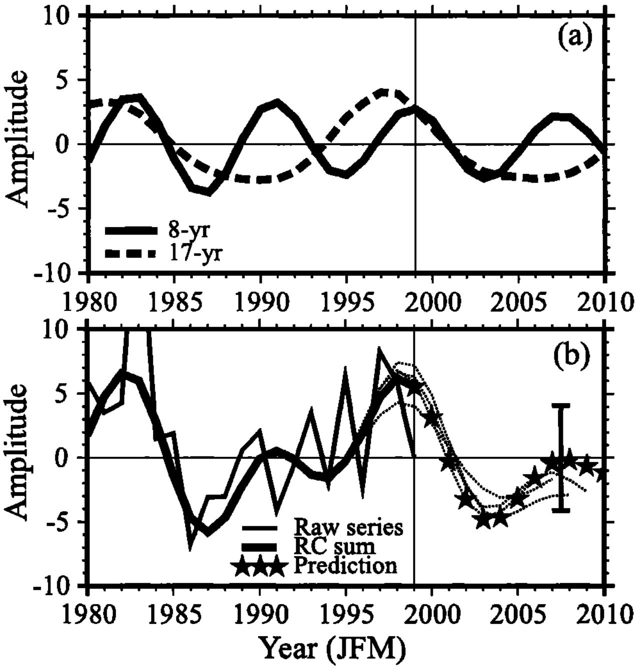

Figure 5. The RCs 1–2 and 3–4 computed over 1904–99 with M = 30, plotted 1980–99, together with their predictions (5 LP coefficients) made from 1999. (a) Individual RC sums and predictions, (b) combined sum (thick solid line) and prediction (stars), and raw JFM flow anomalies (thin line). The thin dotted curves in panel (b) show four predictions starting in 1995, 1996, 1997 and 1998 respectively. Units: 10^3 m^3s^{-1}.

6. A prediction

Figure 5 shows a prediction made with the Corrientes time series updated to March 1999, using RCs computed over the 1904–99 series. Linear prediction is applied to RCs 1–2 (8 yr) and RCs 3–4 (17 yr) computed with $M = 30$, and the results (panel a) summed to give the final prediction (panel b). Both the 17-yr and 8-yr components exhibit substantial amplitudes into the future (panel a). The forecast commencing in 1999 (stars) predicts decreasing flows, and thus a higher probability of drought in years 2002–2006. This prediction is robust to changes in the starting year, as shown by the four thin dotted curves in panel b. The sum of the two RC pairs (panel b, heavy solid line) tracks the raw data series, with the difference between the two curves characteristic of ENSO time scales. The "error bar" in Fig. 5b spans $\pm 2\sigma$ of ENSO streamflow variability that is not included in the forecast, given by the ENSO RCs in Fig. 2. The predicted ebb in 2003–2004 is larger than that expected from a moderate La Niña event.

7. Summary and conclusions

Each of the 17-yr, 8-yr and ENSO oscillatory components of the Paraná river at Corrientes (Fig. 2) is found to be associated with modest but statistically significant changes in the probability distribution of monthly flows (Table 1).

Computing the EOFs "in sample" from the entire series, the predictability of RC *phase* is quite high for the 17- and 8-yr components in terms of anomaly correlation hindcast skill (Fig. 3). Using rigorous out-of-sample validation, we demonstrate statistically significant equitable threat scores for the 8-yr component up to four years in advance for below-normal summer flows (Fig. 4). Flood years appear to be less predictable.

Applying the technique in true forecast mode to the the 8- and 17-yr components predicts an increased probability of low Paraná streamflows lasting until 2006, assuming stationarity in the weak sense. The strong predicted minimum in 2003–2004 is associated with large negative in-phase excursions in the 8- and 17-yr RCs, attaining an amplitude comparable to that found during strong ENSO conditions. The present results underline the potential importance of decadal-scale streamflow climatic fluctuations, and indicate that these may be partially predictable. Although the predictability due to ENSO is found to be negligible at interannual lead times, decadal modulation of ENSO teleconnections may be important, as found in over North America by [*Gershunov and Barnett*, 1998].

Acknowledgments. We are grateful to M. Ghil and A. Saunders for helpful discussions, and a reviewer for constructive comments that improved the manuscript. This work was supported by NOAA grants NA86GPO289 and NA76GPO511. This is publication no. 5667 of UCLA's IGPP.

References

Allen, M.R., and L.A. Smith, Monte Carlo SSA: detecting irregular oscillations in the presence of coloured noise. *J. Climate, 9,* 3373-3404, 1996.

Gershunov, A., and T. P. Barnett, Interdecadal modulation of ENSO teleconnections. *Bull. Amer. Meteor. Soc., 79,* 2715-2725, 1998.

Depetris, P. J., S. Kempe, M. Latif, and W. G. Mook, ENSO-controlled flooding in the Paran'a river 1904–1991. *Naturwissenschaften, 83,* 127-129, 1996.

Dettinger, M.D., C.M. Strong, W. Weibel, M. Ghil, and P. Yiou, Software for singular spectrum analysis of noisy time series. *Eos Trans. AGU, 76(2),* pp12,14,21, 1995.

Dettinger, M. D., D. R. Cayan, and K. T. Redmond, United States Streamflow Probabilities based on Forecasted La Niña, Winter-Spring 2000. *Experimental Long-Lead Forecast Bulletin, 8(4),* 57-59.

Ghil, M., and N. Jiang, Recent forecast skill for the El Niño/Southern Oscillation. *Geophys. Res. Lett., 25,* 171-174, 1998.

Ghil, M., M. Kimoto, and J. D. Neelin, Nonlinear dynamics and predictability in the atmospheric sciences. *Rev. Geophys., 29,* suppl. 46-55, 1991.

Keppenne, C. L., and M. Ghil, Adaptive filtering and prediction of the southern oscillation index. *J. Geophys. Res., 97,* 20449-20454, 1992.

Mechoso, C.R., and G. Perez-Iribarren, Streamflow in southeastern South America and the Southern Oscillation. *J. Climate, 5,* 1535-1539, 1992.

Press, W. H., B. P. Flannery, S. A. Teukolsky, and W. T. Vetterling, Numerical Recipes, Cambridge University Press, New York, 818 pp.

Schaefer, J. T., The critical success index as an indicator of warning skill. *Wea. Forecasting, 5,* 570-575, 1990.

Robertson, A. W., and C. R. Mechoso, Interannual and decadal cycles in river flows of southeastern South America. *J. Climate, 11,* 2570-2581, 1998.

Robertson, A. W., and C. R. Mechoso, Interannual and interdecadal variability of the South Atlantic Convergence Zone. *Mon. Wea. Rev., 128,* 2947-2957, 2000.

Valdés, J. B., D. Entekhabi, H.-M. Shin, and H.-H. Hsieh, An evaluation of the impact of ENSO on the discharges of the Salt River, Arizona. *Proc. 26th Ann. Conf. ASCE Water Resources Planning and Management Division,* Tempe AZ, 1999.

Vautard, R., and M. Ghil, Singular spectrum analysis in nonlinear dynamics with applications to paleoclimatic time series. *Physica D, 58,* 95-126, 1989.

Vautard, R., P. Yiou, and M. Ghil, Singular spectrum analysis: A toolkit for short, noisy, chaotic signals. *Physica D., 58,* 95-126, 1992.

C. R. Mechoso, A. W. Robertson UCLA Dept. Atmospheric Sciences, 405 Hilgard Ave., Los Angeles, CA 90095-1565. (e-mail: mechoso@atmos.ucla.edu, andy@atmos.ucla.edu)

N. O. Garcia, Universidad Nacional del Litoral, C.C. 217, Ciudad Universitaria, 3000 Santa Fe, Argentina. (e-mail: nogarcia@fich.unl.edu.ar)

(Received August 10, 2000; accepted June 6, 2001.)